Elastodynamics based Modelling of Acoustic Emission for Earlier Bearing Damage Detection

Anurag Bhattacharyya[1], Krishnan Thyagarajan[2], Jin Yan[3], Kevin Pintong[4], Qiushu Chen[5], Joseph Lee[6], Peter Kiesel[7], and Kai Goebel[8]

[1,8] *Intelligent Systems Laboratory, Future Concepts Division, SRI International, Palo Alto, CA, 94304, USA*
anurag.bhattacharyya@sri.com
kai.goebel@sri.com

[2, 3, 4, 5, 6, 7] *Hardware Research Technology Labs, Future Concepts Division, SRI International, Palo Alto, CA, 94304, USA*
krishnan.thyagarajan@sri.com

ABSTRACT

It is crucial for many applications to detect bearing damage as early as possible to allow for scheduling of maintenance with lead times that minimize operational disruption. State of the practice is the detection of spalling but damage initiates prior to spalling as subsurface and surface cracks. Such damage is much harder to detect and to model. This study proposes a unique application of the nanofrictional Prandtl-Tomlinson model to predict macroscopic acoustic emission (AE) signals that occur at cracked interfaces under relative motion. The study integrates large deformation modelling of structures with elastodynamic simulations to investigate early AE signals generated under different bearing rotational speeds. Experimental studies are carried out to measure acoustic vibrations from metal-metal surface friction using fiber optic sensors and compared to those predicted by the model. Broad agreement of results highlights the validity of this framework.

1. INTRODUCTION

It is forecast that by 2026, the digital twin market will grow to a size of more than $ 48 billion (Abraham et al., 2022). With the advent of the industry 4.0, development of digital twins has been under a considerable amount of focus to avoid faults or breakdowns that can affect the operational output and quality. Through digital twinning, manufacturers can both tweak designs and monitor assets so they can predict when any parts might need replacing. As a result, there has been an increased shift from reactive maintenance to proactive maintenance. One of the most important machinery components is the bearing which is critical to operation of virtually all rotating equipment. The current state-of-the-art in damage detection of bearings leaves a gap between the initiation of fatigue cracks and the eventual detection of crack networks. Closing this gap has the potential to save costs related to maintenance, labor, and downtime.

Studies have shown that due to repeated loading, high-cycle fatigue initiates subsurface cracks in the bearing inner-race. These subsurface cracks eventually form a crack network leading to spalling. The current state-of-the-art techniques can detect AE signals generated mostly after the formation of crack network. Currently used techniques to determine bearing failure rely on monitoring acceleration, velocity, or displacement. Low frequency eddy current measurements (0-6 kHz) rely on displacement detection, laser doppler vibrometers (2 Hz – 12 kHz) measure velocity differences, while AE detection (50-300 kHz), shock pulse, accelerometers, and spike energy detection (20 kHz – 350 kHz) detect acceleration changes due to bearing damage. It is posited that early signs crack initiation are manifested at higher frequencies relative to signals generated by spalling. Therefore, one requires the capacity to measure across a larger frequency spectrum. Currently, most deployed detection platforms interrogate into small brackets of frequency and there is no single system that covers the entire range.

While AE signal detection has been suggested for bearings, the majority that work focuses on damage resulting from artificially seeded defects (Cockerill et al., 2016)(Al-Balushi, Addali, Charnley, & Mba, 2010). However, these represent an already advanced stage of damage. Both Data-driven and Physics-informed methods have investigated bearing damage detection (Fuentes, Dwyer-Joyce, Marshall, Wheals, & Cross, 2020)(Lu et al., 2023). Some investigations have looked into computational simulation of AE signals focused on crack propagation(Faisal Haider & Giurgiutiu, 2019). Studies have also been performed to determine the generation

of AE signals due to rubbing of cracked interfaces using the moment tensor concept (Joseph & Giurgiutiu, 2020). There exist still however, a few challenges for data-driven or hybrid frameworks especially for bearing prognostics. Indeed, most of the data-sets available for bearing damage are based on artificially induced damage that do not provide information on the initial fatigue-induced crack formation stages. Similarly, the majority of physics-informed methods lack the computational fidelity required to model the high-cycle fatigue and damage initiation.

This study aims to address the questions: 1) can we computationally model and simulate the early AE signals generated during the formation of subsurface fatigue cracks under different bearing operating conditions to enable early damage detection and 2) is there any single platform that can be used to measure signals across a large frequency spectrum (Hz to MHz)?

2. MODELLING ACOUSTIC EMISSION FROM CRACKED INTERFACES UNDER RUBBING

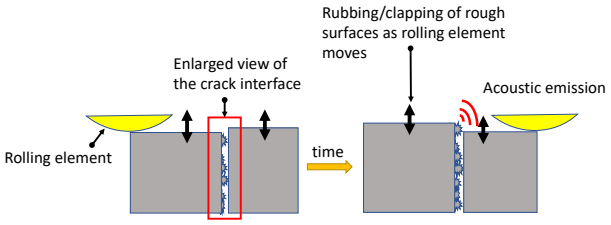

Figure 1. Emission of AE signals from rubbing of cracked interface as the ball bearing passes over the cracked interface.

The formation of damage in bearings typically initiates from defects or imperfections in the material or surface that act as stress raisers. These defects can be present from the manufacturing process or can accumulate over time during operation. During the manufacturing process, defects or imperfections can be introduced into the material's matrix. These defects can include inclusions, voids, dislocations, or other microstructural irregularities. Voids (or vacancies) in the matrix of a material can migrate or move under applied mechanical loads. It is possible for these voids to accumulate at grain boundaries when their movement is inhibited. As a result, grain boundaries can act as preferred sites for the nucleation and accumulation of defects, including voids or vacancies. When the bearing is subjected to operational loads and stresses, the presence of these matrix defects can lead to localized stress concentration. As the bearing continues to operate under cyclic loading conditions, the localized stress concentration at the matrix defects can exceed the material's fatigue strength or fracture toughness. This can lead to the formation of microscopic cracks. Once the initial cracks have formed, they tend to propagate or grow under the influence of the cyclic stresses and the presence of the surrounding defects. As the cracks continue to propagate, they may coalesce or join together, forming larger cracks or surface defects. Eventually, this can lead to the formation of spalls, which are localized areas where material has been dislodged or removed from the bearing surface. When a lightly damaged bearing is under motion, the cracked interfaces rub/clap. This releases shear stress energy which is manifested as acoustic emission(AE) signals. Fig. 1 shows a conceptual representation of the process. As the bearing rolls over the cracked interface, the surfaces rub against one another causing the generation of AE signals. The simultaneous presence of motion and rubbing between the surfaces inspired the use of Prandtl-Tomlinson (PT) model. The PT model provides a way to simulate the stick-slip frictional motion characteristics through a simple spring mass system. Vanossi et al. (Vanossi, Manini, Urbakh, Zapperi, & Tosatti, 2013) showed that the qualitative conclusions drawn from the model retain their validity in more advanced models and MD simulations. The rubbing between two cracked interfaces is modeled as a single solid with a maximum dimension of l dragged across an undulating surface with a velocity (v). The model can be used to simulate various stages of crack evolution by changing the length l. Various speed of operation of the bearing can be correlated with the velocity parameter, v, at which the body is dragged across the surface as shown in Fig. 2. The surface (S) over

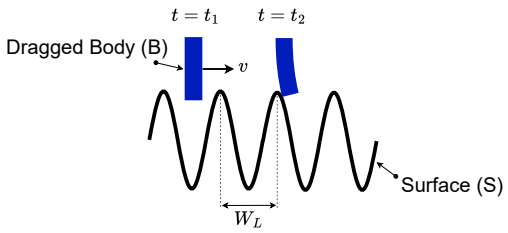

Figure 2. PT inspired model of a cracked interface under motion. The body B is dragged across the surface S with a constant velocity v.

which the solid body is dragged, is modelled as a sinusoidal function with wavelength (W_L). For this study, the value of the wavelength parameter (W_L) is taken to be 0.1 mm. The body is initially given a displacement ($d = \delta$). In this study, the value of parameter $\delta = 0.01$ mm. A displacement-controlled large deformation based finite element analysis is performed to determine the forcing amplitude (F_{amp}). The forcing amplitude is then multiplied with a clipped sinusoidal function to form the external force function (F_t) which is used to simulate the effect of the body being dragged across sinusoidal surface. The reason for using a clipped forcing function is the actual physical interaction occurring between the body dragged (B) across the surface and the surface profile (S). It can be observed that the external force on B initiates at the time of first contact with S. The amplitude at the first time of contact is the minimum amplitude of force that

is experienced by B. This amplitude becomes maximum as B passes interacts with the peak of S and then gradually the amplitude reduces to zero as the dragged body passes the surface peak. Thus the external force acts on B only during a small amount while the interaction occurs. This is simulated as a clipped sinusoidal forcing function as represented by (1). For this study, the clipping threshold is taken as 80% of the F_{amp} value. This value can be tailored to simulate the effects of friction between the two interacting bodies, amount of lubrication available or the amount of clamping force between interacting solids.

$$\begin{cases} F_t = F_{amp}\sin(ft), & \text{if } F_t \geq 0.8F_{amp} \\ 0, & \text{otherwise} \end{cases} \tag{1}$$

Where,

$$f = \frac{v}{W_L} \tag{2}$$

The obtained time-dependent loading (F_t) is shown in Fig. 3. After the evaluation of the external dynamical force (F_t) acting on the structure, an elastodynamics problem is solved using the α-Method (Hilber-Hughes-Taylor Method), to introduce numerical damping, without degrading the order of accuracy with $\alpha = -0.3$. The material used for the simulation is structural steel with Young's Modulus value of 200 GPa. The problem formulation and solution were computed using a custom code generated in MATLAB. The time dependent loading is applied on a square domain ("domain" is used here in the sense of physical space under investigation) as shown in Fig. 4a and the displacement of the structure in the y-direction is obtained from the simulation as shown in Fig. 4b. A fast-Fourier transform (FFT) is taken of this temporal signature to generate a single-sided amplitude spectrum with a sampling window parameter ($F_s = 10^8$) as shown in Fig. 3.

To correlate the motion of the bearing with the motion of the cracked interface, it is assumed that every time a bearing passes over the cracked interface, the cracked domains rub against each other. This assumption can be explained from the fact that the rotational motion of the ball bearings is not a pure rotational motion. This is due to the presence of friction and other external forces due to lubrication or radial loading. The presence of frictional forces between the ball bearing and the inner race, in the presence of a cracked interface, will cause the cracked surfaces to collide. At a more microscopic level, the collision between the cracked surfaces will give rise to motion not only in the direction of the collision but also in perpendicular direction to the collision. This is due to the presence of surface asperities along the cracked interface. The motion in the perpendicular direction will be amplified due to the free boundary conditions near the inner race surface. This will give rise to a rubbing/sliding motion between the cracked interfaces. For this study the ratio (R) between the radius of the bearing and that of the shaft is taken as approximately 11 for a wind turbine (Yucesan & Viana, 2019). This provides us with the ball rotational speed (ω_b). The ball rotational speed is used to evaluate frequency (f). For an example, if the shaft rotational speed is 50 rpm, the maximum ball rotational speed will be given by (3).

$$\omega_b = R \times 50 = 550 \ \text{ rpm} \tag{3}$$

The frequency of the ball passing the cracked interface will then be 9.1 Hz. The velocity of the body dragged across the surface can then be evaluated using (2) as shown in (4).

$$v = 9.1 \times W_L = 9.1 \times 0.1 = 0.91 \ \text{ mm /s} \tag{4}$$

3. PRELIMINARY RESULTS

Initial studies were performed with a square shaped domain with a time-dependent force (F_t) as shown in Fig. 3. The

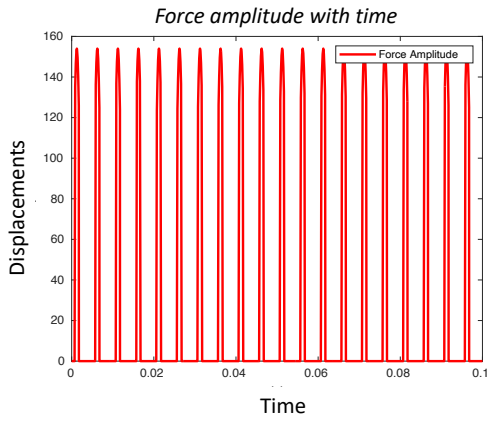

Figure 3. Time dependent force (F_t) acting on the body (B)

square domain is discretized with a coarse mesh. The dynamical simulations are performed for domain capable of undergoing large deformation (geometric nonlinearity) with linear elasticity model. The domain size for simulation was based

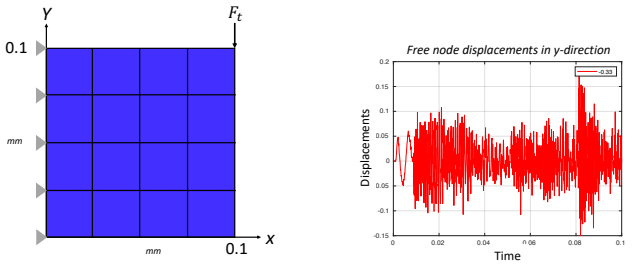

(a) a (b) b

Figure 4. Domain and simulation results of the elastodynamic analysis representing a cracked interface under motion

upon a study (Singh, Pulikollu, Hawkins, & Smith, 2017)

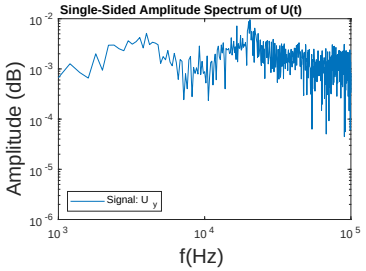

Figure 5. Amplitude spectrum of the displacement-vs-time signal for a square domain

that investigated the cracks formed in wind turbine gearbox bearings. From the study, we took the average domain to be of size $0.1\text{mm} \times 0.1\text{mm}$ as shown in Fig.4a. The FFT of the transient displacement response, as shown in Fig. 4b, is shown in Fig. 5. The geometric nonlinearity allows for a frequency magnification of about 90 times, when the output structural frequencies are compared with the frequency of the input force.

To mimic fatigue-based cracked interface profiles more closely (Yu et al., 2021), the domain shape was changed to a triangular one as shown in Fig. 6. The dynamical response of the triangular domain was investigated for two different lengths of simulation time. The elastodynamical simulations were run for a time (T) of 0.1s and 1s to gauge the effects of different operational times. The results show that as the domain is vibrated for longer duration, even though the order of the maximum frequencies remain the same (O (10^5)), the amplitude and shape of the signal changes significantly as shown in Fig. 7. To account for the effects of bearing

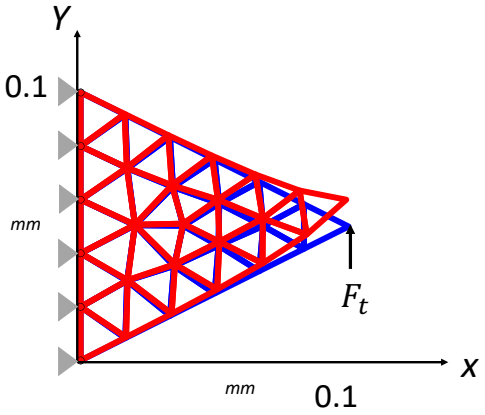

Figure 6. Large deformation of triangular domain to mimic crack-interface tribology

rotational speed on the frequency of the emitted AE signals, large-deformation elastodynamics simulation is carried for

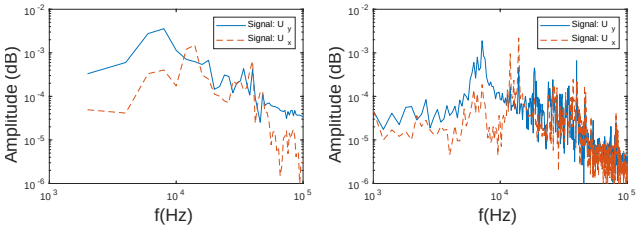

(a) $t = 0.1$s (b) $t = 1$s

Figure 7. The frequency response for triangular domain for $t = 0.1$s and $t = 1$s

different values of velocity (v) parameters. The frequency spectrum of the temporal signals are shown in Fig. 8. The

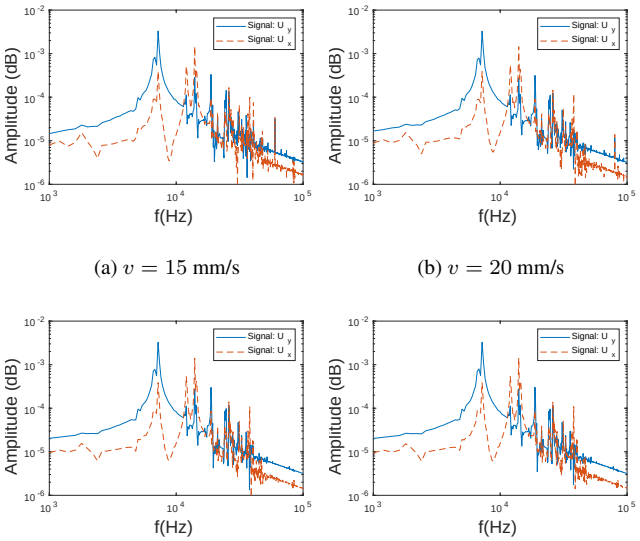

(a) $v = 15$ mm/s (b) $v = 20$ mm/s

(c) $v = 45$ mm/s (d) $v = 50$ mm/s

Figure 8. Fast-Fourier Transform of temporal signals obtained from elasto-dynamic simulations for different values of velocities

analysis was conducted for a range of velocity values. The correlation obtained between the velocities and the order of the maximum frequency obtained for each velocity is plotted in Fig. 8. The relation between velocity of bearing operations and frequency of signal emitted for large velocities, $v = 100$ mm/s and $v = 500$ mm/s is also obtained and shown in Fig. 9. We observe, from Fig. 8 and Fig. 9, that for different bearing operational velocities, the average signal intensity is shifting from $O(10^5)$ towards $O(10^4)$. This can be explained by the fact that the frequency response essentially consists of two components. The first component is the *direct* result of the impact force, and the second component is the *response* to the impact force during the time when no force acts on it. Initially for low velocities, these two components of the

frequency response feed into each other resulting in an increase of the maximum order of the frequency response. As the velocity increases above a certain threshold, as shown in Fig. 9 for $v = 100$ mm/s and $v = 500$ mm/s, the amount of time between two subsequent impact loads decrease, causing a decrease in the response contribution of the frequency component and thereby decreasing the maximum order of the frequency output.

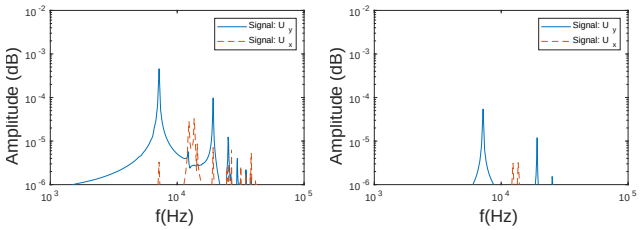

(a) $v = 100$ mm/s (b) $v = 500$ mm/s

Figure 9. Fast-Fourier Transform of temporal signals obtained from elasto-dynamic simulations for $v = 100$ mm/s and $v = 500$ mm/s

4. EXPERIMENTAL RESULTS AND DISCUSSION

The aim of the experiments was to establish initial experimental measurements on metal-metal friction leading to the creation of AE signals and to compare our findings between experiments and simulations. To that end, we sought a system that mimics the above simulations of two rough metal surfaces rubbing against each other. The measurement setup consisted of an end mill (2 and 4 flute) that was used to mill blocks of different metals at varying velocities (or revolutions per minute) as shown in Fig.10. While this is not the same it is sufficiently equivalent to the region of the crack interface as seen in Fig. 2.

In particular, we argue that there is equivalence in frictional contact and energy dissipation mechanisms. All surfaces involved in these processes have surface roughness and asperities (microscopic peaks and valleys). In the case of an end mill, the grains create a rough surface, while in a damaged bearing, the crack surfaces tend to be rough and irregular due to the fracture process. During the milling process, the abrasive grains on the end mill are in frictional contact with the metal work-piece, causing material removal through a combination of plowing, cutting, and fracture mechanisms. Similarly, in a damaged bearing, the two crack surfaces are in frictional contact, and their relative motion generates energy dissipation through friction and wear processes. In addition, in both cases, a significant portion of the energy input is dissipated through friction and elastoplastic deformation processes. In milling, the energy is supplied by the motion of

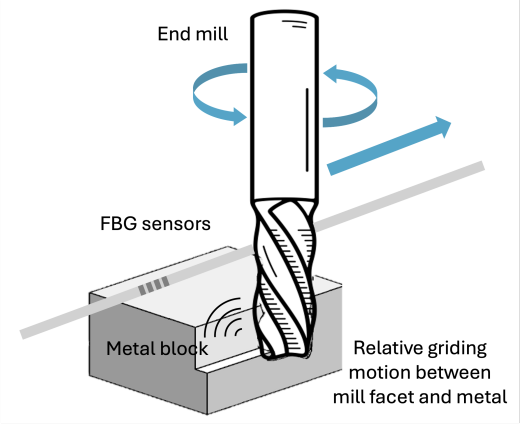

Figure 10. Schematic of the frictional interaction between the end mill and the metal block, that generates the acoustic waves. These waves are picked up by the FBG sensors placed near the interaction point.

the mill against the metal block, while in a damaged bearing, the energy comes from the relative motion of the crack surfaces due to the applied load and operational conditions. During the milling process, the grains on the end facet of the mill are in frictional contact with the metal work-piece, causing material removal through a combination of plowing, cutting, and fracture mechanisms. Similarly, in a damaged bearing, the two crack surfaces are in frictional contact, and their relative motion generates energy dissipation through friction and wear processes. In addition, in both cases, a significant portion of the energy input is dissipated through friction and elastoplastic deformation processes. In milling, the energy is supplied by the relative motion of the milling end, while in a damaged bearing, the energy comes from the relative motion of the crack surfaces due to the applied load and operational conditions. It is important to note that while the fundamental mechanisms of frictional contact and energy dissipation are similar, there are also significant differences in the specific details and scales involved. The milling process is typically a controlled material removal operation (essentially a shearing operation that separates material), while the motion of crack surfaces in a damaged bearing is an undesirable phenomenon that leads to further degradation and failure (mostly rubbing of surfaces with some growth in crack size) . Nevertheless, the comparison of these two processes can provide insights into the tribological and material behavior at the interface, allowing for the application of similar analytical and modeling approaches to understand and predict the phenomena involved.

To measure the AE signals, we used custom Fiber Bragg Gratings (FBGs) etched on to optical fibers as displacement sensors. FBGs have the capacity to pick up minute changes in strain caused by acoustic waves triggered in the metal upon metal-metal interaction, which are manifested as very small displacements of the fiber. Our sensitive readout system en-

ables us to detect displacements down to 30 fm (Overton, 2011)(Kiesel et al., 2007) (1400 nm – 1700 nm). We designed a compact transimpedance amplifier with an amplification of 106 V/A and bandwidth of 58kHz (3dB frequency). The amplifier chip itself was able to provide amplification up to a bandwidth of 120KHz but in order to improve the noise performance we set the bandwidth to 60kHz. The amplifier is based on a Precision, Very Low Noise, Low Input Bias Current, Wide Bandwidth JFET Operational Amplifiers from Analog Devices. For our measurements, the fibers were affixed onto one of the metal surfaces using epoxy, to measure strain changes at different wavelengths in the range of 1400 nm - 1700 nm. We studied the impact on the measured frequencies of the AE, for varying metal-metal relative velocities (or revolutions per minute). Two examples of employing a stainless-steel drill to measure the acoustic emission vibrations picked up by the fiber optic sensors mounted on a copper plate or an aluminum plate are shown in Fig. 11. For the measurement, the end mill was carefully lowered onto the metal of interest, within a 2 inch distance from the FBG sensors. As can be seen, for the different RPM speeds across the two metals there is a strong series of peaks between 10^4 and 10^5 Hz, but no significant variation in the frequencies of the emitted AE signals across the different cases. This compares well with what is seen in the modeling of metal-metal friction rubbing in Fig. 8 and Fig. 9. One of the expected reasons of the lack of variation could be the fact that the velocities under consideration are far lower than the velocity of sound in the metals and thus small input variations do not affect the AE signals greatly. However, this also clearly shows that to detect the beginning of damage of two metal surfaces grinding against each other, measuring signals in the aforementioned frequency range may be beneficial.

The FBG sensors are well-suited for such applications due to their compactness, low-cost, low susceptibility to electromagnetic interference (EMI), capacity to multiplex sensors and easy installation across hard-to-reach sections of instrumentation. Another significant advantage of FBG sensors is that they allow measurements across a large bandwidth of frequencies from Hz to MHz. For our application example, we are especially interested in the higher frequencies and used a variable operational amplifier to control the frequency bandwidth of measurement on our chipaccordingly. This means that we can detect slow degradation of vibrating metallic parts across a large frequency range, giving insight into various kinds of potential fault modes.

5. CONCLUSIONS

This study proposes the use of the nanofrictional Prandtl-Tomlinson model to predict the frequencies that occur at cracked interfaces of early bearing damage. According to the model, frequencies are expected in the acoustic emission (AE) region, confirming observations in the field. The study considers different bearing rotational speeds and integrates large deformation modelling of structures with elastodynamic simulations. Initial experimental studies on metal-metal surface friction use fiber optic sensors that can capture AE signals. The results, although preliminary in nature, agree with those predicted by the model. The ability to detect bearing damage at this early stage has the promise to significantly increase the prognostic horizon for bearing failure.

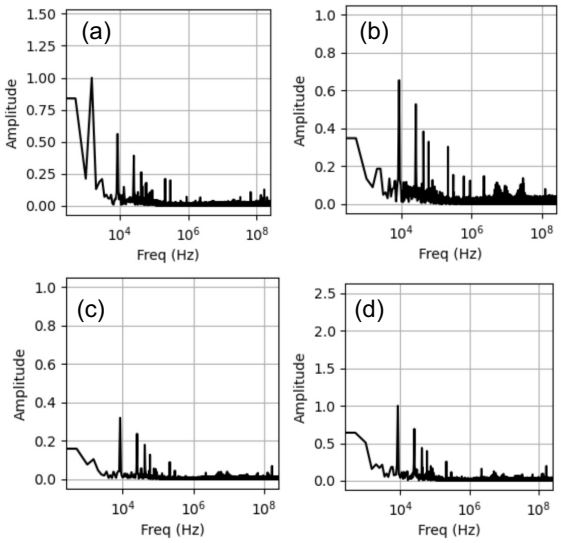

Figure 11. Fiber optic strain measurements picking up acoustic emission signals generated from the interaction of two metal surfaces for different metals and relative velocities: (a) copper-stainless steel (4000 RPM), (b) copper-stainless steel (6000 RPM), (c) aluminum-stainless steel (5000 RPM) and (d) aluminum-stainless steel (7000 RPM). The presence of the strongest signals between 10^4 and 10^5 Hz in both experiments and simulations is clearly seen.

REFERENCES

Abraham, J. C., Cruz, G., Cubela, S., Lajous, T., Rowshankish, K., Tiwari, S., & Zemmel, R. (2022, Oct). *Digital twins: From one twin to the enterprise metaverse.* McKinsey Company. Retrieved from https://www.mckinsey.com/capabilities/mckinsey-digital/our-insights/digital-twins-from-one-twin-to-the-enterprise-metaverse

Al-Balushi, K. R., Addali, A., Charnley, B., & Mba, D. (2010, September). Energy Index technique for detection of Acoustic Emissions associated with incipient bearing failures. *Applied Acoustics*, *71*(9), 812–821. Retrieved 2024-02-23, from https://www.sciencedirect.com/science/article/pii/S0003682X10000873 doi: 10.1016/j.apacoust.2010.04.006

Cockerill, A., Clarke, A., Pullin, R., Bradshaw, T., Cole,

P., & Holford, K. (2016, November). Determination of rolling element bearing condition via acoustic emission. *Proceedings of the Institution of Mechanical Engineers, Part J: Journal of Engineering Tribology*, *230*(11), 1377–1388. Retrieved 2024-02-24, from https://doi.org/10.1177/1350650116638612 (Publisher: IMECHE) doi: 10.1177/1350650116638612

Faisal Haider, M., & Giurgiutiu, V. (2019, May). Theoretical and numerical analysis of acoustic emission guided waves released during crack propagation. *Journal of Intelligent Material Systems and Structures*, *30*(9), 1318–1338. Retrieved 2024-02-24, from https://doi.org/10.1177/1045389X18798948 (Publisher: SAGE Publications Ltd STM) doi: 10.1177/1045389X18798948

Fuentes, R., Dwyer-Joyce, R. S., Marshall, M. B., Wheals, J., & Cross, E. J. (2020, March). Detection of sub-surface damage in wind turbine bearings using acoustic emissions and probabilistic modelling. *Renewable Energy*, *147*, 776–797. Retrieved 2024-02-23, from https://www.sciencedirect.com/science/article/pii/S0960148119312066 doi: 10.1016/j.renene.2019.08.019

Joseph, R., & Giurgiutiu, V. (2020, May). Acoustic emission (AE) fatigue-crack source modeling and simulation using moment tensor concept. In *Sensors and Smart Structures Technologies for Civil, Mechanical, and Aerospace Systems 2020* (Vol. 11379, pp. 214–225). SPIE. Retrieved 2024-02-23, from https://www.spiedigitallibrary.org/conference-proceedings-of-spie/11379/113791J/Acoustic-emission-AE-fatigue-crack-source-modeling-and-simulation-using/10.1117/12.2559958.full doi: 10.1117/12.2559958

Kiesel, P., Beck, M., Schmidt, O., Johnson, N., Bassler, M., Ecke, W., … Bartelt, H. (2007, October). Compact and fast interrogation unit for fiber Bragg grating sensors. In *Photonics in the Transportation Industry: Auto to Aerospace* (Vol. 6758, pp. 81–85). SPIE. Retrieved 2024-02-24, from https://www.spiedigitallibrary.org/conference-proceedings-of-spie/6758/67580A/Compact-and-fast-interrogation-unit-for-fiber-Bragg-grating-sensors/10.1117/12.734869.full doi: 10.1117/12.734869

Lu, H., Pavan Nemani, V., Barzegar, V., Allen, C., Hu, C., Laflamme, S., … Zimmerman, A. T. (2023, May). A physics-informed feature weighting method for bearing fault diagnostics. *Mechanical Systems and Signal Processing*, *191*, 110171. Retrieved 2024-02-23, from https://www.sciencedirect.com/science/article/pii/S088832702300078X doi: 10.1016/j.ymssp.2023.110171

Overton, G. (2011, January). *FIBER-OPTIC-SENSORS: Miniature read-out sensor resolves wavelength changes to 50 fm.* Retrieved 2024-02-24, from https://www.laserfocusworld.com/detectors-imaging/article/16548058/fiber-optic-sensors-miniature-read-out-sensor-resolves-wavelength-changes-to-50-fm

Singh, H., Pulikollu, R. V., Hawkins, W., & Smith, G. (2017, May). Investigation of Microstructural Alterations in Low- and High-Speed Intermediate-Stage Wind Turbine Gearbox Bearings. *Tribology Letters*, *65*(3), 81. Retrieved 2024-02-24, from https://doi.org/10.1007/s11249-017-0861-5 doi: 10.1007/s11249-017-0861-5

Vanossi, A., Manini, N., Urbakh, M., Zapperi, S., & Tosatti, E. (2013, April). Modeling friction: From nanoscale to mesoscale. *Reviews of Modern Physics*, *85*(2), 529–552. Retrieved 2024-02-23, from http://arxiv.org/abs/1112.3234 (arXiv:1112.3234 [cond-mat]) doi: 10.1103/RevModPhys.85.529

Yu, X., Lin, X., Tan, H., Hu, Y., Zhang, S., Liu, F., … Huang, W. (2021). Microstructure and fatigue crack growth behavior of inconel 718 superalloy manufactured by laser directed energy deposition. *International Journal of Fatigue*, *143*, 106005.

Yucesan, Y. A., & Viana, F. A. (2019). Wind turbine main bearing fatigue life estimation with physicsinformed neural networks. In *Annual conference of the phm society* (Vol. 11, pp. 1–14).

BIOGRAPHIES

Anurag Bhattacharyya is a research scientist in the Intelligent Systems Laboratory at SRI International. Anurag obtained his Ph.D. and M.S. degree in Aerospace Engineering from the University of Illinois Urbana Champaign in 2021 and 2017, respectively. He received his B.Tech. degree in Mechanical Engineering from the National Institute of Technology, Durgapur, India in 2014. In 2013, he was the only recipient of the CERN summer fellowship from the Mechanical Engineering department. His current research is focused on digital design and manufacturing. His areas of expertise include nonlinear material modeling, topology optimization, finite element analysis, smart materials and 3D/4D printing techniques. Prior to joining PARC, his research was centered around design and fabrication of multi-functional adaptive structures leveraging geometric and material nonlinearities. He designed self-actuated mechanisms by integrating structural design optimization framework with novel time-dependent adjoint sensitivity formulation for multi-material shape memory polymers harnessing

high-performance computing. He also worked as a production engineer for a battery manufacturing conglomerate and design engineer for a major consultancy firm in India.

Krishnan Thyagarajan leads the cross-disciplinary Sensors, Devices and Systems (SDS) group that covers various aspects of sensing technologies ranging from sensing to making sense in the domains of energy, infrastructure protection, healthcare, and manufacturing. Krishnan obtained his Ph.D. and M.S. in Applied Physics and Photonics from the École Polytechnique Fédérale de Lausanne (EPFL), Switzerland and a B.S. with honors in Physics from the University of Delhi, India. His research work is funded both by federal agencies (DARPA, NIH, ARPA-E, DOE, DTRA) and commercial partners, and aims to deliver on novel science and technology directly impacting society. His expertise includes smart sensors, energy and material supply resilience, patient-centered diagnostics, hardware security (classical and quantum), and scalable optoelectronic manufacturing technologies. He was a Swiss National Science Foundation Fellow at the Thomas J. Watson Lab of Applied Physics and the Kavli Nanoscience Institute at Caltech, Pasadena. There, funded by AFOSR, ONR, DOE, SNSF, Samsung, and Sony, he worked on metamaterials, metasurfaces, quantum nanophotonics, and set a record for the world's first attojoule plasmonic optical modulator. He has authored more than 40 publications, and 25 patents and is the co-founder of a PARC spin-off company for electromagnetic supercooling (EverCase Inc.).

Kai Goebel, PhD, is director of the Intelligent Systems Lab. Dr. Goebel has a Ph.D. in mechanical engineering from UC Berkeley and a degree of Diplom-Ingenieur from TU Munich. He joined PARC in 2019 and has been a lab director since 2020. Dr. Goebel has more than 25 years' experience leading, conducting, and managing research in corporate and government organizations. His research interests are in advancing AI for resilience, autonomous systems, and systems health management. He has transitioned technology into practice, including to the International Space Station, Small Sats, to Space Launch Systems, commercial airlines, FAA, UTM, aircraft engines operations, and into a commercial spinout for predictive maintenance. Prior to joining SRI-PARC, Dr. Goebel worked at NASA Ames Research Center where he was the Area Lead for Discovery and Systems Health. There he founded the Prognostics Center of Excellence which spearheaded development of prognostic techniques, metrics, and generation of publicly available run-to-failure datasets for various components. Dr. Goebel started his professional career at GE Corporate RD where he developed and fielded data-driven analytics applications for manufacturing systems, energy applications, medical systems, and transportation systems. He holds 20 patents and has published more than 400 papers in the field. Dr. Goebel was an adjunct professor at Rensselaer Polytechnic Institute and guest professor at University of Cincinnati. He still holds an Adjunct Professor appointment at Lulea Technical University. He is a member of ASME, IEEE, SAE, AAAI; co-founder and fellow of the Prognostics and Health Management Society; and associate editor of the International Journal of PHM.